JACS
JOURNAL OF THE AMERICAN CHEMICAL SOCIETY
Cite This: J. Am. Chem. Soc. 2018, 140, 16042−16047
Communication
pubs.acs.org/JACS

Selective CO_2 Reduction Catalyzed by Single Cobalt Sites on Carbon Nitride under Visible-Light Irradiation

Peipei Huang,[†] Jiahao Huang,[‡] Sebastian A. Pantovich,[†] Alexander D. Carl,[§] Thomas G. Fenton,[†] Christine A. Caputo,[†] Ronald L. Grimm,[§] Anatoly I. Frenkel,*[,‡,⊥] and Gonghu Li*[,†]

[†]Department of Chemistry, University of New Hampshire, Durham, New Hampshire 03857, United States
[‡]Department of Materials Science and Chemical Engineering, Stony Brook University, Stony Brook, New York 11794, United States
[§]Department of Chemistry & Biochemistry, Worcester Polytechnic Institute, Worcester, Massachusetts 01609, United States
[⊥]Division of Chemistry, Brookhaven National Laboratory, Upton, New York 11973, United States

Supporting Information

ABSTRACT: Framework nitrogen atoms of carbon nitride (C_3N_4) can coordinate with and activate metal sites for catalysis. In this study, C_3N_4 was employed to harvest visible light and activate Co^{2+} sites, without the use of additional ligands, in photochemical CO_2 reduction. Photocatalysts containing single Co^{2+} sites on C_3N_4 were prepared by a simple deposition method and demonstrated excellent activity and product selectivity toward CO formation. A turnover number of more than 200 was obtained for CO production using the synthesized photocatalyst under visible-light irradiation. Inactive cobalt oxides formed at relatively high cobalt loadings but did not alter product selectivity. Further studies with X-ray absorption spectroscopy confirmed the presence of single Co^{2+} sites on C_3N_4 and their important role in achieving selective CO_2 reduction.

The past few years witnessed increasing interest in hybrid photosynthetic systems that couple molecular catalysts with robust surfaces for solar fuel production.[1−6] Light-absorbing semiconductors,[7−19] electrode surfaces,[20−26] and other solid-state materials[27−30] have been employed as support for molecular CO_2-reduction catalysts. Among the light-absorbing semiconductors, some have wide bandgaps,[9] and their activation requires the use of UV irradiation that accounts for less than 5% of the solar spectrum. Only a few semiconductors with relatively narrow bandgaps can harvest visible light for subsequent photoexcited electron transfer to the surface-bound molecular catalysts for CO_2 reduction.[7,17,19] Metal−ligand complexes are often employed as molecular catalysts. These complexes usually render excellent reactivity and product selectivity, but their ligands may be expensive or difficult to synthesize in large scales. This present work employs graphitic carbon nitride (C_3N_4) to harvest visible light and activate single Co^{2+} sites, without the use of additional ligands, in selective CO_2 reduction (Figure 1a).

Recently, C_3N_4 has emerged as a semiconductor capable of mediating photocatalysis under visible-light irradiation.[31] This polymeric material has been investigated in solar water splitting[32] and CO_2 reduction.[33] In photocatalytic CO_2 reduction, C_3N_4 has been studied as a photocatalyst alone,[34]

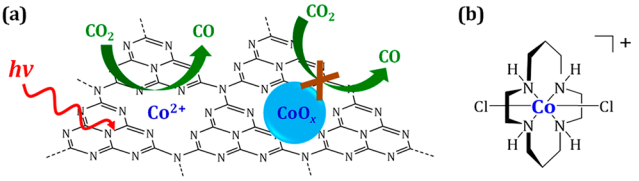

Figure 1. (a) Schematic of photocatalytic CO_2 reduction mediated by a single Co^{2+} site on C_3N_4; (b) molecular structure of a macrocyclic cobalt catalyst.

or coupled with catalysts including metal nanoparticles[35−37] and metal−ligand complexes[14−17,38] for enhanced solar fuel production. Theoretical studies by Gao and co-workers suggest that efficient visible-light CO_2 reduction can be achieved using single Pd and Pt atoms supported on C_3N_4.[39] However, no experimental work has been reported regarding selective solar CO_2 reduction using single-metal-site catalysts in the absence of additional ligands.

In the present study, single Co^{2+} sites are prepared on C_3N_4 via a simple deposition method to achieve selective CO_2 reduction under visible-light irradiation. Activation of the single Co^{2+} sites on C_3N_4 is likely through Co−N coordination, as in a well-known molecular catalyst, [Co(cyclam)Cl_2]Cl where cyclam is 1,4,8,11-tetraazacyclotetradecane (denoted "Co-cyclam", structure shown in Figure 1b). This macrocyclic cobalt catalyst is often used with *p*-terphenyl as a photosensitizer in CO_2 reduction under UV irradiation.[40,41] We also present spectroscopic evidence for the presence of single Co^{2+} sites and their essential role in photocatalysis.

The X-ray diffraction pattern of C_3N_4 prepared by pyrolysis of urea is shown in Figure 2a. Deposition of Co^{2+} sites on C_3N_4 was achieved by mixing $CoCl_2$ with C_3N_4 in acetonitrile, followed by microwave heating in the presence of triethylamine (TEA). In our study, TEA was employed to facilitate the deposition of Co^{2+} on C_3N_4. Cobalt loadings of the synthesized materials (denoted "Co^{2+}@C_3N_4") increased almost linearly with the amount of $CoCl_2$ used in synthesis (see Figure S1 in the Supporting Information). Approximately

Received: September 26, 2018
Published: November 10, 2018

DOI: 10.1021/jacs.8b10380
J. Am. Chem. Soc. 2018, 140, 16042−16047

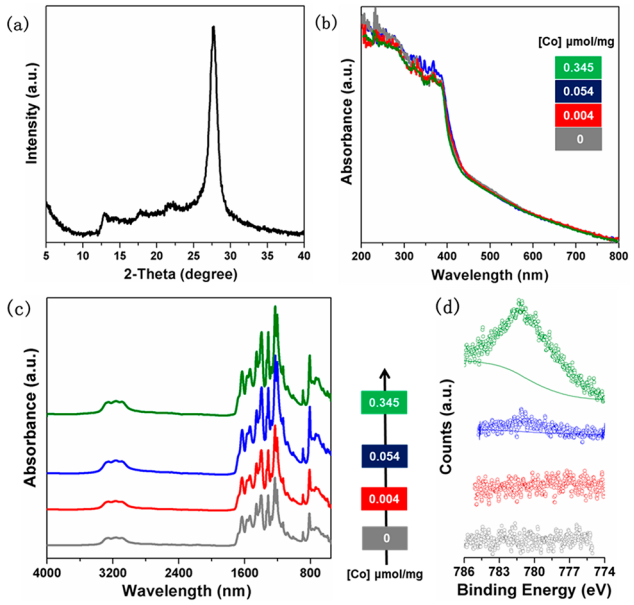

Figure 2. (a) X-ray powder diffraction pattern of bare C_3N_4; (b) optical spectra, (c) infrared spectra, and (d) X-ray photoelectron spectra of bare C_3N_4 and different $Co^{2+}@C_3N_4$ samples.

45% of $CoCl_2$ used in synthesis was successfully deposited on C_3N_4. Cobalt loadings in this work varied between 0.004 and 0.430 μmol Co^{2+} per 1 mg C_3N_4. When the microwave synthesis was carried out in the absence of TEA, however, the highest cobalt loading obtained was 0.016 μmol/mg even when a large excess of $CoCl_2$ was used in synthesis (Figure S1).

The optical spectrum of bare C_3N_4 features significant photoresponse in the visible region (400−800 nm, Figure 2b), similar to that of C-doped C_3N_4 reported in the literature (Figure S2).[42,43] Deposition of Co^{2+} on C_3N_4 resulted in a negligible change in its optical spectrum. The infrared spectra of the $Co^{2+}@C_3N_4$ samples are almost identical to that of bare C_3N_4(Figure 2c). In addition, no morphological changes were observed upon deposition of Co^{2+} (Figure S3a−d). The presence of Co^{2+} sites in the $Co^{2+}@C_3N_4$ samples is seen in their X-ray photoelectron spectra, as indicated by a peak at 781 eV associated with the Co $2p_{3/2}$ transition (Figure 2d).[44] Microscopic mapping revealed uniform distribution of cobalt on C_3N_4 (Figure S3f).

The $Co^{2+}@C_3N_4$ samples were tested for photocatalytic CO_2 reduction in acetonitrile containing triethanolamine as a sacrificial electron donor. A halogen lamp was used to provide photons with wavelength greater than 350 nm (see lamp output spectrum in Figure S4). Under the experimental conditions employed in this study, CO and H_2 were detected as major products in CO_2 reduction using the $Co^{2+}@C_3N_4$ samples. Negligible CO production was observed using bare C_3N_4 (Figure S5). Interestingly, a significant amount of CO was generated in CO_2 reduction using a mixture of $CoCl_2$ and C_3N_4. At the same cobalt loading, the amount of CO produced by $Co^{2+}@C_3N_4$ is about 5 times greater than that by the mixture of $CoCl_2$ and C_3N_4 (Figure S5). This comparison highlights the importance of the deposition process, in which Co−N coordination likely occurred, in activating the Co^{2+} sites on C_3N_4.

The effect of cobalt loading on the photocatalytic activity of $Co^{2+}@C_3N_4$ was further examined under the same experimental conditions. Significant CO production was observed even at cobalt loadings lower than 0.010 μmol/mg (Figure 3a).

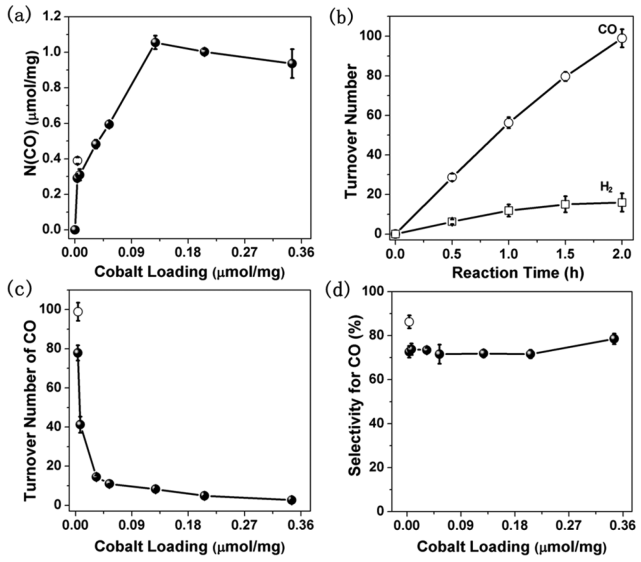

Figure 3. (a) Amounts of CO produced after CO_2 reduction for 2 h using different $Co^{2+}@C_3N_4$ samples; (b) example of TONs for CO and H_2 production as a function of reaction time; and (c) TONs of CO and (d) selectivity toward CO production after CO_2 reduction for 2 h. The open cycle represents a $Co^{2+}@C_3N_4$ sample prepared in the absence of TEA. Error bars were calculated based on triplicate data points.

The amount of CO generated in CO_2 reduction increased linearly with cobalt loading until it reached 0.128 μmol/mg. Further increase in cobalt content resulted in a slight decrease in the amount of CO produced. Quantum yields up to 0.40% were obtained for CO production using the synthesized materials (Tables S1 and S2).

The effect of cobalt loading was also investigated by comparing turnover numbers (TONs), which were calculated based on the amount of product and the amount of cobalt present in the reaction suspension. Figure 3b shows TON for CO and H_2 production over reaction time using a $Co^{2+}@C_3N_4$ sample prepared in the absence of TEA. After CO_2 reduction for 2 h, the TON for CO formation was measured to be ∼100. TONs for CO decreased drastically as the cobalt loading was increased (Figure 3c), suggesting the existence of single-site catalysis at low cobalt loadings. At relatively high loadings, a significant portion of cobalt likely exists in the form of inactive cobalt oxides. An interesting observation in CO_2 reduction using $Co^{2+}@C_3N_4$ is that product selectivity appeared to be independent of the cobalt loading, as can be seen from Figure 3d. Therefore, the inactive cobalt component in $Co^{2+}@C_3N_4$ did not promote undesired competing reactions, including H_2 production.

The $Co^{2+}@C_3N_4$ samples demonstrated excellent activity under visible-light irradiation (λ > 420 nm, see Figure S4). A TON greater than 200 was obtained after CO_2 reduction after 24 h using a $Co^{2+}@C_3N_4$ sample (Figure S6). Isotopic studies clearly showed that CO was produced as a result of CO_2 reduction (Figure S6, inset). The $Co^{2+}@C_3N_4$ samples also demonstrated reasonable stability, as indicated by significant CO production using recycled $Co^{2+}@C_3N_4$ samples in photocatalysis (Figure S7). In addition, no morphological

DOI: 10.1021/jacs.8b10380
J. Am. Chem. Soc. 2018, 140, 16042−16047

changes were observed for the $Co^{2+}@C_3N_4$ samples before and after photocatalysis (Figures S8 and S9).

The unique structure of C_3N_4 (Figure 1a) allows it to serve as a "ligand", in which framework N atoms coordinate with and activate metal sites for catalysis. This concept of catalysis at single metal sites was previously explored electrocatalytically using metal-doped C_3N_4[45,46] and metal/N-doped carbon-based electrodes.[47−54] Similar efforts were reported in photocatalytic water oxidation[55,56] and H_2 evolution[57,58] using single Co sites on C_3N_4. However, visible-light CO_2 reduction using single metal sites on C_3N_4 has not been previously observed in the absence of additional coordinating ligand. Our study is the first example demonstrating the use of single Co^{2+} sites on C_3N_4 for selective CO_2 reduction under visible-light irradiation.

The nature of single Co^{2+} sites and their role in photocatalysis using $Co^{2+}@C_3N_4$ was further investigated with X-ray absorption spectroscopy using two samples with cobalt loadings of 0.016 μmol/mg (denoted "low-$Co^{2+}@C_3N_4$") and 0.430 μmol/mg (denoted "high-$Co^{2+}@C_3N_4$"). For this study, a control sample was prepared by depositing $CoCl_2$ on SiO_2 in the presence of TEA (denoted "CoO_x/SiO_2", cobalt loading 0.254 μmol/mg, Figure S10). Figure 4 shows

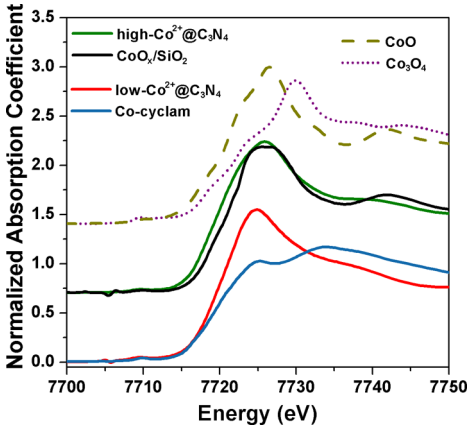

Figure 4. Normalized Co K-edge XANES spectra of Co-cyclam, high-$Co^{2+}@C_3N_4$, low-$Co^{2+}@C_3N_4$, CoO_x/SiO_2, and two standard Co compounds.

the Co K-edge X-ray absorption near edge structure (XANES) spectra of these samples as well as Co-cyclam in the powder form. Comparison among the XANES spectra indicates that the cobalt species in CoO_x/SiO_2 and Co-cyclam are at higher oxidation states than those in high-$Co^{2+}@C_3N_4$ and low-$Co^{2+}@C_3N_4$ (Figure S11). The oxidation state of cobalt in both $Co^{2+}@C_3N_4$ samples remained at 2+, consistent with similar Co-doped C_3N_4 materials reported in the literature.[55,59] In prior studies by others[57,60] and one of the coauthors,[61] a shoulder feature along the rising edge around 7715 eV was observed in the XANES of Co-porphyrins having the four-coordinate square-planar structure. This shoulder feature is not present in the XANES of our samples, indicating Co^{2+} is not in the same plane as the flat framework of N atoms in C_3N_4.

The XANES spectral shape for low-$Co^{2+}@C_3N_4$ is different from those of CoO and Co_3O_4, likely due to the coordination of Co^{2+} with N atoms in the C_3N_4 framework. In contrast, the XANES spectral shapes of high-$Co^{2+}@C_3N_4$ and CoO_x/SiO_2 are similar to that of CoO, consistent with the presence of CoO in both samples (Figure 4). The presence of cobalt oxide in $Co^{2+}@C_3N_4$ at relatively high cobalt loadings was confirmed with X-ray photoelectron spectroscopy (Figure S12).

The extended X-ray absorption fine structure (EXAFS) spectra of these samples are shown in Figure 5. The k-range

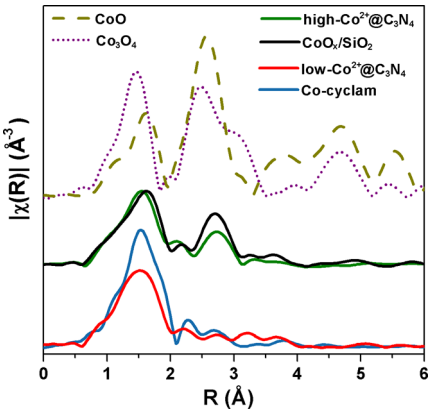

Figure 5. Fourier transform magnitude of k^2-weighted Co K-edge EXAFS spectra of Co-cyclam, high-$Co^{2+}@C_3N_4$, low-$Co^{2+}@C_3N_4$, CoO_x/SiO_2, and two standard Co compounds.

from 2 to 11 $Å^{-1}$ and k^2 weighting were used in all Fourier transforms. Similar to Co-cyclam, the spectra of both high-$Co^{2+}@C_3N_4$ and low-$Co^{2+}@C_3N_4$ have a peak around 1.55 Å (uncorrected for the photoelectron phase shift), which indicates coordination of Co^{2+} with N atoms in these samples. A peak at around 2.7 Å corresponding to Co−Co bond in CoO structure is present in the EXAFS spectra of high-$Co^{2+}@C_3N_4$ and CoO_x/SiO_2, with the former having lower intensity. This comparison indicates that (1) the cobalt oxide species in high-$Co^{2+}@C_3N_4$ has a similar structure to that in CoO_x/SiO_2; and (2) the cobalt oxide species in high-$Co^{2+}@C_3N_4$ has a lower coordination number at Co and/or higher disorder than that in CoO_x/SiO_2, possibly because the size of cobalt oxides in high-$Co^{2+}@C_3N_4$ is smaller than in CoO_x/SiO_2, despite significantly higher cobalt loading in high-$Co^{2+}@C_3N_4$ than in CoO_x/SiO_2.

The spectra shown in Figure 5 demonstrate that in cobalt species in low-$Co^{2+}@C_3N_4$, no Co−O−Co contribution can be detected, consistent with the conclusion obtained from the XANES data (Figure 4). Therefore, cobalt species in this sample exist as isolated, single sites with a coordination environment similar to that of Co-cyclam. In comparison, the high-$Co^{2+}@C_3N_4$ sample contains cobalt oxides, which are inactive in photocatalytic CO_2 reduction under the experimental conditions employed in this study (Figure 1a).

In summary, we have successfully prepared single Co^{2+} sites on C_3N_4 for use in selective CO_2 reduction under visible-light irradiation. Photocatalysis and spectroscopic studies clearly demonstrated the formation of single Co^{2+} sites and their important role in achieving selective CO_2 reduction. Our work contributes to the field of solar fuels by providing a rare example of CO_2-reduction photocatalysts featuring single catalytic sites based on earth-abundant transition metals.

■ ASSOCIATED CONTENT

Supporting Information

The Supporting Information is available free of charge on the ACS Publications website at DOI: 10.1021/jacs.8b10380.

DOI: 10.1021/jacs.8b10380
J. Am. Chem. Soc. 2018, 140, 16042−16047

Experimental details on materials, catalyst synthesis, materials characterization, X-ray absorption spectroscopy, photocatalytic testing; estimated quantum yields; and supporting figures (PDF)

AUTHOR INFORMATION

Corresponding Authors

*anatoly.frenkel@stonybrook.edu

*gonghu.li@unh.edu

ORCID

Christine A. Caputo: 0000-0002-0925-8679

Ronald L. Grimm: 0000-0003-0407-937X

Anatoly I. Frenkel: 0000-0002-5451-1207

Gonghu Li: 0000-0002-2924-3597

Notes

The authors declare no competing financial interest.

ACKNOWLEDGMENTS

This material is based upon work supported by the U.S. Department of Energy (DOE), Office of Science, Office of Basic Energy Sciences under Award Number DE-SC0016417 to C.C. and G.L. (catalyst synthesis, characterization and photocatalysis), and the U.S. National Science Foundation under grant CBET-1510810 to G.L. (infrared studies). A.I.F. acknowledges support of the U.S. DOE Grant No. DE-FG02-03ER15476 for X-ray absorption spectroscopy measurements and analysis part of this research, and support by the Laboratory Directed Research and Development Program through LDRD 18-047 of Brookhaven National Laboratory under U.S. DOE Contract No. DE-SC0012704 for initiating his research in single atom catalysts. This research used beamline 7-BM (QAS) of the National Synchrotron Light Source II, a U.S. DOE Office of Science User Facility operated for the DOE Office of Science by Brookhaven National Laboratory under Contract No. DE-SC0012704. Beamline operations were supported in part by the Synchrotron Catalysis Consortium (U.S. DOE, Office of Basic Energy Sciences, Grant No. DE-SC0012335). We thank Dr. Steven Ehrlich for help with the beamline measurements at the QAS beamline. We are grateful to Prof. Xiaowei Teng, Prof. Nan Yi, and Dr. Scott Greenwood for assistance in various aspects of experiments.

REFERENCES

(1) Tran, P. D.; Wong, L. H.; Barber, J.; Loo, J. S. C. Recent advances in hybrid photocatalysts for solar fuel production. *Energy Environ. Sci.* **2012**, *5*, 5902−5918.

(2) Kumar, B.; Llorente, M.; Froehlich, J.; Dang, T.; Sathrum, A.; Kubiak, C. P. Photochemical and photoelectrochemical reduction of CO_2. *Annu. Rev. Phys. Chem.* **2012**, *63*, 541−569.

(3) White, J. L.; Baruch, M. F.; Pander, J. E., III; Hu, Y.; Fortmeyer, I. C.; Park, J. E.; Zhang, T.; Liao, K.; Gu, J.; Yan, Y.; Shaw, T. W.; Abelev, E.; Bocarsly, A. B. Light-Driven Heterogeneous Reduction of Carbon Dioxide: Photocatalysts and Photoelectrodes. *Chem. Rev.* **2015**, *115*, 12888−12935.

(4) Sato, S.; Arai, T.; Morikawa, T. Toward Solar-Driven Photocatalytic CO_2 Reduction Using Water as an Electron Donor. *Inorg. Chem.* **2015**, *54*, 5105−5113.

(5) Windle, C. D.; Reisner, E. Heterogenised Molecular Catalysts for the Reduction of CO_2 to Fuels. *Chimia* **2015**, *69*, 435−441.

(6) Louis, M. E.; Fenton, T. G.; Rondeau, J.; Jin, T.; Li, G. Solar CO_2 Reduction Using Surface-Immobilized Molecular Catalysts. *Comments Inorg. Chem.* **2016**, *36*, 38−60.

(7) Sato, S.; Morikawa, T.; Saeki, S.; Kajino, T.; Motohiro, T. Visible-Light-Induced Selective CO_2 Reduction Utilizing a Ruthenium Complex Electrocatalyst Linked to a p-Type Nitrogen-Doped Ta_2O_5 Semiconductor. *Angew. Chem., Int. Ed.* **2010**, *49*, 5101−5105.

(8) Suzuki, T. M.; Tanaka, H.; Morikawa, T.; Iwaki, M.; Sato, S.; Saeki, S.; Inoue, M.; Kajino, T.; Motohiro, T. Direct assembly synthesis of metal complex-semiconductor hybrid photocatalysts anchored by phosphonate for highly efficient CO_2 reduction. *Chem. Commun.* **2011**, *47*, 8673−8675.

(9) Jin, T.; Liu, C.; Li, G. Photocatalytic CO_2 reduction using a molecular cobalt complex deposited on TiO_2 nanoparticles. *Chem. Commun.* **2014**, *50*, 6221−6224.

(10) Windle, C. D.; Pastor, E.; Reynal, A.; Whitwood, A. C.; Vaynzof, Y.; Durrant, J. R.; Perutz, R. N.; Reisner, E. Improving the Photocatalytic Reduction of CO_2 to CO through Immobilization of a Molecular Re Catalyst on TiO_2. *Chem. - Eur. J.* **2015**, *21*, 3746−3754.

(11) Won, D.-I.; Lee, J.-S.; Ji, J.-M.; Jung, W.-J.; Son, H.-J.; Pac, C.; Kang, S. O. Highly Robust Hybrid Photocatalyst for Carbon Dioxide Reduction: Tuning and Optimization of Catalytic Activities of Dye/TiO_2/Re(I) Organic-Inorganic Ternary Systems. *J. Am. Chem. Soc.* **2015**, *137*, 13679−13690.

(12) Akimov, A. V.; Asahi, R.; Jinnouchi, R.; Prezhdo, O. V. Photocatalytic CO2 reduction on N-doped Ta2O5 efficient: Insights from nonadiabatic molecular dynamics. *J. Am. Chem. Soc.* **2015**, *137*, 11517−11525.

(13) Liu, C.; Jin, T.; Louis, M. E.; Pantovich, S. A.; Skraba-Joiner, S. L.; Rajh, T.; Li, G. Molecular deposition of a macrocyclic cobalt catalyst on TiO_2 nanoparticles. *J. Mol. Catal. A: Chem.* **2016**, *423*, 293−299.

(14) Lin, J.; Pan, Z.; Wang, X. Photochemical Reduction of CO_2 by Graphitic Carbon Nitride Polymers. *ACS Sustainable Chem. Eng.* **2014**, *2*, 353−358.

(15) Walsh, J. J.; Jiang, C.; Tang, J.; Cowan, A. J. Photochemical CO_2 reduction using structurally controlled g-C_3N_4. *Phys. Chem. Chem. Phys.* **2016**, *18*, 24825−24829.

(16) Kuriki, R.; Matsunaga, H.; Nakashima, T.; Wada, K.; Yamakata, A.; Ishitani, O.; Maeda, K. Nature-Inspired, Highly Durable CO_2 Reduction System Consisting of a Binuclear Ruthenium(II) Complex and an Organic Semiconductor Using Visible Light. *J. Am. Chem. Soc.* **2016**, *138*, 5159−5170.

(17) Cometto, C.; Kuriki, R.; Chen, L.; Maeda, K.; Lau, T.-C.; Ishitani, O.; Robert, M. A Carbon Nitride/Fe Quaterpyridine Catalytic System for Photostimulated CO_2-to-CO Conversion with Visible Light. *J. Am. Chem. Soc.* **2018**, *140*, 7437−7440.

(18) Abdellah, M.; El-Zohry, A. M.; Antila, L. J.; Windle, C. D.; Reisner, E.; Hammarström, L. Time-Resolved IR Spectroscopy Reveals a Mechanism with TiO_2 as a Reversible Electron Acceptor in a TiO_2−Re Catalyst System for CO_2 Photoreduction. *J. Am. Chem. Soc.* **2017**, *139*, 1226−1232.

(19) Kuehnel, M. F.; Orchard, K. L.; Dalle, K. E.; Reisner, E. Selective Photocatalytic CO_2 Reduction in Water through Anchoring of a Molecular Ni Catalyst on CdS Nanocrystals. *J. Am. Chem. Soc.* **2017**, *139*, 7217−7223.

(20) Blakemore, J. D.; Gupta, A.; Warren, J. J.; Brunschwig, B. S.; Gray, H. B. Noncovalent Immobilization of Electrocatalysts on Carbon Electrodes for Fuel Production. *J. Am. Chem. Soc.* **2013**, *135*, 18288−18291.

(21) Weng, Z.; Jiang, J.; Wu, Y.; Wu, Z.; Guo, X.; Materna, K. L.; Liu, W.; Batista, V. S.; Brudvig, G. W.; Wang, H. Electrochemical CO_2 Reduction to Hydrocarbons on a Heterogeneous Molecular Cu Catalyst in Aqueous Solution. *J. Am. Chem. Soc.* **2016**, *138*, 8076−8079.

(22) Rosser, T. E.; Windle, C. D.; Reisner, E. Electrocatalytic and Solar-Driven CO2 Reduction to CO with a Molecular Manganese Catalyst Immobilized on Mesoporous TiO2. *Angew. Chem., Int. Ed.* **2016**, *55*, 7388−7392.

(23) Schreier, M.; Luo, J.; Gao, P.; Moehl, T.; Mayer, M. T.; Grätzel, M. Covalent Immobilization of a Molecular Catalyst on Cu_2O

DOI: 10.1021/jacs.8b10380
J. Am. Chem. Soc. 2018, 140, 16042−16047

Photocathodes for CO_2 Reduction. *J. Am. Chem. Soc.* **2016**, *138*, 1938−1946.
(24) Jin, T.; He, D.; Li, W.; Stanton, C. J.; Pantovich, S. A.; Majetich, G. F.; Schaefer, H. F.; Agarwal, J.; Wang, D.; Li, G. CO_2 reduction with Re(I)-NHC compounds: driving selective catalysis with a silicon nanowire photoelectrode. *Chem. Commun.* **2016**, *52*, 14258−14261.
(25) Zhang, X.; Wu, Z.; Zhang, X.; Li, L.; Li, Y.; Xu, H.; Li, X.; Yu, X.; Zhang, Z.; Liang, Y.; Wang, H. Highly selective and active CO_2 reduction electrocatalysts based on cobalt phthalocyanine/carbon nanotube hybrid structures. *Nat. Commun.* **2017**, *8*, 14675.
(26) Reuillard, B.; Ly, K. H.; Rosser, T. E.; Kuehnel, M. F.; Zebger, I.; Reisner, E. Tuning Product Selectivity for Aqueous CO_2 Reduction with a Mn(bipyridine)-pyrene Catalyst Immobilized on a Carbon Nanotube Electrode. *J. Am. Chem. Soc.* **2017**, *139*, 14425−14435.
(27) Wang, C.; Xie, Z.; deKrafft, K. E.; Lin, W. Doping Metal-Organic Frameworks for Water Oxidation, Carbon Dioxide Reduction, and Organic Photocatalysis. *J. Am. Chem. Soc.* **2011**, *133*, 13445−13454.
(28) McNicholas, B. J.; Blakemore, J. D.; Chang, A. B.; Bates, C. M.; Kramer, W. W.; Grubbs, R. H.; Gray, H. B. Electrocatalysis of CO_2 Reduction in Brush Polymer Ion Gels. *J. Am. Chem. Soc.* **2016**, *138*, 11160−11163.
(29) Kramer, W. W.; McCrory, C. C. L. Polymer coordination promotes selective CO_2 reduction by cobalt phthalocyanine. *Chem. Sci.* **2016**, *7*, 2506−2515.
(30) Liu, C.; Dubois, K. D.; Louis, M. E.; Vorushilov, A. S.; Li, G. Photocatalytic CO_2 Reduction and Surface Immobilization of a Tricarbonyl Re(I) Compound Modified with Amide Groups. *ACS Catal.* **2013**, *3*, 655−662.
(31) Wang, X.; Chen, X.; Thomas, A.; Fu, X.; Antonietti, M. Metal-Containing Carbon Nitride Compounds: A New Functional Organic-Metal Hybrid Material. *Adv. Mater.* **2009**, *21*, 1609−1612.
(32) Liu, J.; Liu, Y.; Liu, N.; Han, Y.; Zhang, X.; Huang, H.; Lifshitz, Y.; Lee, S.-T.; Zhong, J.; Kang, Z. Metal-free efficient photocatalyst for stable visible water splitting via a two-electron pathway. *Science* **2015**, *347*, 970−974.
(33) Fang, Y.; Wang, X. Photocatalytic CO_2 conversion by polymeric carbon nitrides. *Chem. Commun.* **2018**, *54*, 5674−5687.
(34) Di, T.; Zhu, B.; Cheng, B.; Yu, J.; Xu, J. A direct Z-scheme g-C_3N_4/SnS_2 photocatalyst with superior visible-light CO_2 reduction performance. *J. Catal.* **2017**, *352*, 532−541.
(35) Shi, H.; Chen, G.; Zhang, C.; Zou, Z. Polymeric g-C_3N_4 Coupled with $NaNbO_3$ Nanowires toward Enhanced Photocatalytic Reduction of CO_2 into Renewable Fuel. *ACS Catal.* **2014**, *4*, 3637−3643.
(36) Shi, G.; Yang, L.; Liu, Z.; Chen, X.; Zhou, J.; Yu, Y. Photocatalytic reduction of CO_2 to CO over copper decorated g-C_3N_4 nanosheets with enhanced yield and selectivity. *Appl. Surf. Sci.* **2018**, *427*, 1165−1173.
(37) Li, H.; Gao, Y.; Xiong, Z.; Liao, C.; Shih, K. Enhanced selective photocatalytic reduction of CO_2 to CH_4 over plasmonic Au modified g-C_3N_4 photocatalyst under UV−vis light irradiation. *Appl. Surf. Sci.* **2018**, *439*, 552−559.
(38) Maeda, K.; An, D.; Kumara Ranasinghe, C. S.; Uchiyama, T.; Kuriki, R.; Kanazawa, T.; Lu, D.; Nozawa, S.; Yamakata, A.; Uchimoto, Y.; Ishitani, O. Visible-light CO_2 reduction over a ruthenium(ii)-complex/C_3N_4 hybrid photocatalyst: the promotional effect of silver species. *J. Mater. Chem. A* **2018**, *6*, 9708−9715.
(39) Gao, G.; Jiao, Y.; Waclawik, E. R.; Du, A. Single Atom (Pd/Pt) Supported on Graphitic Carbon Nitride as an Efficient Photocatalyst for Visible-Light Reduction of Carbon Dioxide. *J. Am. Chem. Soc.* **2016**, *138*, 6292−6297.
(40) Matsuoka, S.; Yamamoto, K.; Ogata, T.; Kusaba, M.; Nakashima, N.; Fujita, E.; Yanagida, S. Efficient and selective electron mediation of cobalt complexes with cyclam and related macrocycles in the p-terphenyl-catalyzed photoreduction of carbon dioxide. *J. Am. Chem. Soc.* **1993**, *115*, 601−609.
(41) Ogata, T.; Yanagida, S.; Brunschwig, B. S.; Fujita, E. Mechanistic and Kinetic Studies of Cobalt Macrocycles in a Photochemical CO_2 Reduction System: Evidence of Co-CO_2 Adducts as Intermediates. *J. Am. Chem. Soc.* **1995**, *117*, 6708−6716.
(42) Che, W.; Cheng, W.; Yao, T.; Tang, F.; Liu, W.; Su, H.; Huang, Y.; Liu, Q.; Liu, J.; Hu, F.; Pan, Z.; Sun, Z.; Wei, S. Fast Photoelectron Transfer in (C_{ring})−C_3N_4 Plane Heterostructural Nanosheets for Overall Water Splitting. *J. Am. Chem. Soc.* **2017**, *139*, 3021−3026.
(43) Xu, Q.; Jiang, C.; Cheng, B.; Yu, J. Enhanced visible-light photocatalytic H_2-generation activity of carbon/g-C_3N_4 nanocomposites prepared by two-step thermal treatment. *Dalton Trans.* **2017**, *46*, 10611−10619.
(44) Mao, Z.; Chen, J.; Yang, Y.; Wang, D.; Bie, L.; Fahlman, B. D. Novel g-C_3N_4/CoO Nanocomposites with Significantly Enhanced Visible-Light Photocatalytic Activity for H_2 Evolution. *ACS Appl. Mater. Interfaces* **2017**, *9*, 12427−12435.
(45) Li, X.; Bi, W.; Chen, M.; Sun, Y.; Ju, H.; Yan, W.; Zhu, J.; Wu, X.; Chu, W.; Wu, C.; Xie, Y. Exclusive Ni-N_4 Sites Realize Near-Unity CO Selectivity for Electrochemical CO_2 Reduction. *J. Am. Chem. Soc.* **2017**, *139*, 14889−14892.
(46) Zheng, Y.; Jiao, Y.; Zhu, Y.; Cai, Q.; Vasileff, A.; Li, L. H.; Han, Y.; Chen, Y.; Qiao, S. Z. Molecule-Level g-C_3N_4 Coordinated Transition Metals as a New Class of Electrocatalysts for Oxygen Electrode Reactions. *J. Am. Chem. Soc.* **2017**, *139*, 3336−3339.
(47) Kattel, S.; Wang, G. A density functional theory study of oxygen reduction reaction on Me−N_4 (Me = Fe, Co, or Ni) clusters between graphitic pores. *J. Mater. Chem. A* **2013**, *1*, 10790−10797.
(48) Kattel, S.; Wang, G. Reaction Pathway for Oxygen Reduction on FeN_4 Embedded Graphene. *J. Phys. Chem. Lett.* **2014**, *5*, 452−456.
(49) Ju, W.; Bagger, A.; Hao, G. P.; Varela, A. S.; Sinev, I.; Bon, V.; Roldan Cuenya, B.; Kaskel, S.; Rossmeisl, J.; Strasser, P. Understanding activity and selectivity of metal-nitrogen-doped carbon catalysts for electrochemical reduction of CO_2. *Nat. Commun.* **2017**, *8*, 944.
(50) Bi, W.; Li, X.; You, R.; Chen, M.; Yuan, R.; Huang, W.; Wu, X.; Chu, W.; Wu, C.; Xie, Y. Surface Immobilization of Transition Metal Ions on Nitrogen-Doped Graphene Realizing High-Efficient and Selective CO_2 Reduction. *Adv. Mater.* **2018**, *30*, No. e1706617.
(51) Pan, F.; Deng, W.; Justiniano, C.; Li, Y. Identification of champion transition metals centers in metal and nitrogen-codoped carbon catalysts for CO_2 reduction. *Appl. Catal., B* **2018**, *226*, 463−472.
(52) Pan, F.; Zhang, H.; Liu, K.; Cullen, D.; More, K.; Wang, M.; Feng, Z.; Wang, G.; Wu, G.; Li, Y. Unveiling Active Sites of CO_2 Reduction on Nitrogen-Coordinated and Atomically Dispersed Iron and Cobalt Catalysts. *ACS Catal.* **2018**, *8*, 3116−3122.
(53) Yan, C.; Li, H.; Ye, Y.; Wu, H.; Cai, F.; Si, R.; Xiao, J.; Miao, S.; Xie, S.; Yang, F.; Li, Y.; Wang, G.; Bao, X. Coordinatively unsaturated nickel−nitrogen sites towards selective and high-rate CO_2 electroreduction. *Energy Environ. Sci.* **2018**, *11*, 1204−1210.
(54) Pan, Y.; Lin, R.; Chen, Y.; Liu, S.; Zhu, W.; Cao, X.; Chen, W.; Wu, K.; Cheong, W.-C.; Wang, Y.; Zheng, L.; Luo, J.; Lin, Y.; Liu, Y.; Liu, C.; Li, J.; Lu, Q.; Chen, X.; Wang, D.; Peng, Q.; Chen, C.; Li, Y. Design of Single-Atom Co−N_5 Catalytic Site: A Robust Electrocatalyst for CO_2 Reduction with Nearly 100% CO Selectivity and Remarkable Stability. *J. Am. Chem. Soc.* **2018**, *140*, 4218−4221.
(55) Zhang, G.; Huang, C.; Wang, X. Dispersing molecular cobalt in graphitic carbon nitride frameworks for photocatalytic water oxidation. *Small* **2015**, *11*, 1215−1221.
(56) Zhang, G.; Zang, S.; Lin, L.; Lan, Z.-A.; Li, G.; Wang, X. Ultrafine Cobalt Catalysts on Covalent Carbon Nitride Frameworks for Oxygenic Photosynthesis. *ACS Appl. Mater. Interfaces* **2016**, *8*, 2287−2296.
(57) Cao, Y.; Chen, S.; Luo, Q.; Yan, H.; Lin, Y.; Liu, W.; Cao, L.; Lu, J.; Yang, J.; Yao, T.; Wei, S. Atomic-Level Insight into Optimizing the Hydrogen Evolution Pathway over a Co1-N4 Single-Site Photocatalyst. *Angew. Chem., Int. Ed.* **2017**, *56*, 12191−12196.

DOI: 10.1021/jacs.8b10380
J. Am. Chem. Soc. 2018, 140, 16042−16047

(58) Chen, P.-W.; Li, K.; Yu, Y.-X.; Zhang, W.-D. Cobalt-doped graphitic carbon nitride photocatalysts with high activity for hydrogen evolution. *Appl. Surf. Sci.* **2017**, *392*, 608−615.
(59) Zou, X.; Huang, X.; Goswami, A.; Silva, R.; Sathe, B. R.; Mikmeková, E.; Asefa, T. Cobalt-Embedded Nitrogen-Rich Carbon Nanotubes Efficiently Catalyze Hydrogen Evolution Reaction at All pH Values. *Angew. Chem.* **2014**, *126*, 4461−4465.
(60) Goswami, M.; Lyaskovskyy, V.; Domingos, S. R.; Buma, W. J.; Woutersen, S.; Troeppner, O.; Ivanović-Burmazović, I.; Lu, H.; Cui, X.; Zhang, X. P.; Reijerse, E. J.; DeBeer, S.; van Schooneveld, M. M.; Pfaff, F. F.; Ray, K.; de Bruin, B. Characterization of Porphyrin-Co(III)-'Nitrene Radical' Species Relevant in Catalytic Nitrene Transfer Reactions. *J. Am. Chem. Soc.* **2015**, *137*, 5468−5479.
(61) Frenkel, A. I.; Kleifeld, O.; Wasserman, S. R.; Sagi, I. Phase speciation by extended x-ray absorption fine structure spectroscopy. *J. Chem. Phys.* **2002**, *116*, 9449−9456.

DOI: 10.1021/jacs.8b10380
J. Am. Chem. Soc. 2018, 140, 16042−16047